

Nuclear Matrix Elements of Second-Forbidden Beta Transitions and the j - j Coupling Model*

P. LIPNIK†

Centre de Physique Nucléaire, Louvain, Belgique

AND

J. W. SUNIER

Department of Physics, University of California, Los Angeles, California

(Received 14 October 1965; revised manuscript received 10 February 1966)

The ratios of nuclear matrix elements compatible with the experimental shape factors of the second-forbidden beta transitions in the decay of Cl^{36} , Fe^{59} , Tc^{99} , I^{129} , Cs^{135} , and Cs^{137} are computed. In each case a solution is found which agrees with the predictions $\int iA_{ij}/\int R_{ij}$ of the conserved vector current theory and is close to the extreme single-particle estimate of $\int i T_{ij}/\int R_{ij}$. Deviations are analyzed by introducing small amounts of configuration mixing. The standard matrix elements $\int R_{ij}/R^2$ are computed and compared to their single-particle estimate.

1. INTRODUCTION

SECOND-forbidden beta transitions have been investigated in the past with the purpose of acquiring information about the nature of the weak interaction.¹⁻³ The main idea of these early studies was to try to reduce the number of unknown parameters on the basis of shell-model considerations in order to select interaction type(s) suitable to the experimental data. Now that our knowledge of the weak interaction has been so much improved, it seems justified to reverse the procedure. Starting from a theoretical formalism which we assume to be essentially correct, we may experimentally determine the nuclear matrix elements of the interaction Hamiltonian which are involved in particular beta transitions. Extensive work along these lines has been carried on in allowed and first-forbidden beta decay during the past few years and has brought valuable information about nuclear structure. Beta transitions of increasing order of forbiddenness are characteristic of particular shell-model states. Their study gives as much information about nuclear structure as the similar case of isomeric gamma transitions. The comparison of experimental data and nuclear models might therefore be easier with highly forbidden beta decays than it is with allowed transitions. The purpose of this work is to establish experimental relations between the nuclear matrix elements occurring in the second forbidden beta transitions, and to compare them with some predictions of the j - j coupling shell model.

In the first part, we define the nuclear matrix elements in a spherical representation and their ratios for single-particle shell-model wave functions. Corrections to these single-particle ratios are given using configuration mixing and j - j coupling. In the second part, we give the complete theoretical function for the spectrum shape factor and the electron longitudinal polarization. In the third part, we compare experimental data to these theoretical functions and compute the nuclear-matrix-element ratios compatible with the experiments. In the last part, we discuss the experimental nuclear-matrix-element ratios in terms of their single-particle estimate and compute some qualitative corrections due to the admixture of a limited number of shell model configurations.

2. NUCLEAR MATRIX ELEMENTS INVOLVED IN A SECOND-FORBIDDEN BETA TRANSITION

2.1. Spherical Representation

It appears convenient to express the nuclear matrix elements of the interaction Hamiltonian in terms of reduced matrix elements of spherical tensor operators.

Following the generally accepted notation⁴ for the tensor product of two tensor operators, we define the operators

$$\mathbf{T}_{KL\gamma}^M = i^L r^L [\boldsymbol{\sigma}_\gamma \times \mathbf{Y}_L]_K^M \quad \gamma=0,1, \quad (1)$$

where $\boldsymbol{\sigma}_\gamma$ and $\boldsymbol{\sigma}_0$ are the Pauli matrices and unity operator in their spherical representation and Y_L is a spherical harmonic of degree L . We expand then the beta decay Hamiltonian ($V-A$) in terms of these

* Supported in part by the U. S. Office of Naval Research under contract Nonr-233(44).

† Chercheur agréé à l'Institut Interuniversitaire des Sciences Nucléaires, Belgique.

¹ D. C. Peaslee, *Phys. Rev.* **91**, 1284 (1953).

² M. Morita, J.-I. Fujita, and M. Yamada, *Progr. Theoret. Phys. (Kyoto)* **10**, 630 (1953).

³ C. S. Wu, in *Beta- and Gamma-Ray Spectroscopy*, edited by K. Siegbahn (North-Holland Publishing Company, Amsterdam, Holland, 1955).

⁴ A. de-Shalit and I. Talmi, *Nuclear Shell Theory* (Academic Press Inc., New York, 1963).

operators and get

$$H_\beta = \sum_{KLM} (-)^{K+M} \int_0^\infty r^2 dr$$

$$\times \left\{ \int d\Omega_N [\psi_f^* (C_V - C_A \gamma_5) (\gamma_5)^\gamma \mathbf{T}_{KL\gamma}^M \tau^+ \psi_i] \right\}_{rN=r}$$

$$\times \left\{ \int d\Omega_L [\psi_e^* (1 + \gamma_5) (\gamma_5)^\gamma \mathbf{T}_{KL\gamma}^{-M} \psi_\nu] \right\}_{rL=r}$$

$$+ \text{H.c.} \quad (2)$$

The subscripts N and L refer to the nucleon and lepton space, respectively, and τ^+ is the isospin operator changing a neutron into a proton.

After the integration over the angles, one is left with reduced nuclear matrix elements defined by

$$\int \psi_f^* (\gamma_5)^\gamma \mathbf{T}_{KL\gamma}^M \tau^\pm \psi_i r^2 dr$$

$$\equiv \langle \alpha_f J_f M_f | (\gamma_5)^\gamma \mathbf{T}_{KL\gamma}^M \tau^\pm | \alpha_i J_i M_i \rangle$$

$$= (-)^{J_f - M_f} \begin{pmatrix} J_f & K & J_i \\ -M_f & M & M_i \end{pmatrix}$$

$$\times \langle \alpha_f J_f | (\gamma_5)^\gamma \mathbf{T}_{KL\gamma} \tau^\pm | \alpha_i J_i \rangle. \quad (3)$$

γ' takes the value $\gamma' = \gamma$ for the vector part of the interaction and $\gamma' = \gamma - 1$ for the axial part. τ^\pm applies for β^\pm decay.

The correspondence between the original notation of Konopinski and Uhlenbeck⁵ and our spherical one is established by comparing the Z component of the Cartesian operator to the $M=0$ component of the corresponding spherical tensor. Table I summarizes that correspondence for the matrix elements occurring in second forbidden beta decay.

2.2. Ratios of the Matrix Elements and Their Single-Particle Estimate

Besides the comparative half-life, all the observables related to beta decay depend only on the ratio of the nuclear matrix elements to an arbitrarily chosen normalization. The fact that relativistic matrix elements contribute to the forbidden decay increases the difficulty of theoretical computations. Fortunately, only one ($\int i\mathbf{A}_{ij}$) contributes to the second-forbidden beta decay. The transformation properties of the corresponding operator \mathbf{A}_{ij} are the same as those of the other Fermi contribution to the interaction Hamiltonian (\mathbf{R}_{ij}). The theory of the conserved vector current in

TABLE I. Nuclear matrix elements of second-forbidden beta decay in Cartesian and spherical notation.

| Cartesian | = Spherical | \times Normalization |
|-------------------------|--|---|
| $\int \mathbf{R}_{ij}$ | $\langle J_f \mathbf{T}_{220} \tau^\pm J_i \rangle$ | $-\left(\frac{8\pi}{15}\right)^{1/2} (2J_i + 1)^{-1/2}$ |
| $\int i\mathbf{T}_{ij}$ | $\langle J_f \mathbf{T}_{221} \tau^\pm J_i \rangle$ | $-\left(\frac{16\pi}{5}\right)^{1/2} (2J_i + 1)^{-1/2}$ |
| $\int i\mathbf{A}_{ij}$ | $\langle J_f \gamma_5 \mathbf{T}_{211} \tau^\pm J_i \rangle$ | $\left(\frac{16\pi}{3}\right)^{1/2} (2J_i + 1)^{-1/2}$ |
| $\int \mathbf{S}_{ijk}$ | $\langle J_f \mathbf{T}_{321} \tau^\pm J_i \rangle$ | $-\left(\frac{96\pi}{5}\right)^{1/2} (2J_i + 1)^{-1/2}$ |

weak interactions enables one to establish a relation between these two matrix elements, and that relation⁶ turns out to be independent of the nuclear potential:

$$\int i\mathbf{A}_{ij} = -\Delta_{\text{CVC}} \xi \int \mathbf{R}_{ij}. \quad (4)$$

$$\Delta_{\text{CVC}} = 2.4 + \frac{1}{\xi} \times \begin{cases} W_0 - 2.5 & \text{for } e^- \text{ decay} \\ W_0 + 2.5 & \text{for } e^+ \text{ decay} \\ \Delta M + 1.5 & \text{for e.c. decay.} \end{cases} \quad (5)$$

In these equations, $2\xi = \alpha Z/R$ is the Coulomb energy of the electron at the nuclear radius R , W_0 is the maximum energy available to beta decay, and ΔM is the mass difference between the decaying nucleus and its daughter, all in units of $m_0 c^2$.

Relations between the other matrix elements can be evaluated within the framework of a particular nuclear model. Among these, the j - j coupling shell model has proved to be a valuable tool, at least to evaluate the nuclear wave functions of odd-mass nuclei, with nearly closed shell configurations. In that coupling scheme, the odd-particle wave function is given by

$$|jm\rangle = i^l R(r) [\chi_{1/2} \times Y_l]_j^m \quad (6)$$

where $\chi_{1/2}$ is the spin eigenfunction, Y_l a spherical harmonic, and $R(r)$ the radial wave function.

The reduced matrix elements discussed under Sec. 2.2, taken between two single-particle states $|j_i\rangle = |l'm'\rangle$ and $|j_f\rangle = |lm\rangle$, read then

$$\langle j_f || \mathbf{T}_{KL\gamma} \tau^\pm || j_i \rangle = i^{L+l-l'} [(2j+1)(2K+1)(2j'+1)]^{1/2}$$

$$\times X(\frac{1}{2} \frac{1}{2} \gamma; l'l'K)$$

$$\times \sqrt{2} (\sqrt{3})^\gamma \langle l || Y_L || l' \rangle F_L, \quad (7)$$

where F_L stands for the radial integral

$$F_L = \int r^{L+2} R(r) R'(r) dr. \quad (8)$$

⁵ E. J. Konopinski and G. E. Uhlenbeck, Phys. Rev. **60**, 308 (1941).

⁶ J.-I. Fujita, Progr. Theoret. Phys. (Kyoto) **28**, 338 (1962).

TABLE II. Single-particle ratios Λ_1 s.p. and Λ_2 s.p.^a

| | | $j=l-\frac{1}{2}$ | $j=l+\frac{1}{2}$ |
|------------------|--|---|---|
| Λ_1 s.p. | $j'=l'-\frac{1}{2}$ $j'=l'+\frac{1}{2}$ | $\begin{pmatrix} - \\ - \end{pmatrix}^S \begin{pmatrix} l-l' \\ l+l'+1 \end{pmatrix}$ | $\begin{pmatrix} - \\ - \end{pmatrix}^{S+1} \begin{pmatrix} l+l'+1 \\ l-l' \end{pmatrix}$ |
| Λ_2 s.p. | $j'=l'-\frac{1}{2}$ | $-\left[\frac{3(l+l'-3)(l-l'+3)(l'-l+3)}{5(l+l'+3)} \right]^{1/2}$ | $-\left[\frac{3(l+l'+4)(l-l'+4)(l+l'-2)}{5(l'-l+2)} \right]^{1/2}$ |
| | $j'=l'+\frac{1}{2}$ | $\left[\frac{3(l+l'+4)(l'-l+4)(l+l'-2)}{5(l-l'+2)} \right]^{1/2}$ | $\left[\frac{3(l+l'+5)(l-l'+3)(l'-l+3)}{5(l+l'-1)} \right]^{1/2}$ |

^a $S=0$ for an odd jumping nucleon; $S=1$ for an even jumping nucleon.

For positron decay, one can use the relation

$$\langle j \| \mathbf{T}_{KL\gamma\tau^-} \| j' \rangle = (-)^{K+j'-j+\gamma} \langle j' \| \mathbf{T}_{KL\gamma\tau^+} \| j \rangle. \quad (9)$$

That formulation enables one to compute the following ratios:

$$\Lambda_{1 \text{ s.p.}} = \frac{\int i \mathbf{T}_{ij}}{\int \mathbf{R}_{ij}} = \sqrt{6} \frac{X(\frac{1}{2} \frac{1}{2} 1; l'l'; j'j'2)}{X(\frac{1}{2} \frac{1}{2} 0; l'l'; j'j'2)}, \quad (10)$$

$$\Lambda_{2 \text{ s.p.}} = \frac{\int \mathbf{S}_{ijk}}{\int \mathbf{R}_{ij}} = 3 \left(\frac{21}{5} \right)^{1/2} \frac{X(\frac{1}{2} \frac{1}{2} 1; l'l'; j'j'3)}{X(\frac{1}{2} \frac{1}{2} 0; l'l'; j'j'2)}.$$

In Table II, the single-particle values Λ_1 s.p. and Λ_2 s.p. are computed as function of the orbital angular momenta l and l' . The results are the same as those given by Rose and Osborn.⁷

2.3. Nuclear Matrix Elements and Configuration Mixing

The matrix element ratios described in the preceding section represent a crude estimate. With more realistic wave functions, the numerical evaluation of Λ_1 and Λ_2 becomes complicated. Although one can always reduce the matrix elements of a single-particle operator (such as one has in the case of beta decay) to a linear combination of single-nucleon reduced matrix elements, several radial integrals are involved and the defined ratios lose their simplicity.

Using configuration mixing and j - j coupling, one can formally write the nuclear wave functions as

$$|i\rangle = \alpha_i |j_n' I_i\rangle_{\text{s.p.}} + \sum \beta_i (j_1' \cdots j_n')$$

$$\times |j_1' j_2' \cdots j_n'; I_i\rangle, \quad (11)$$

$$|f\rangle = \alpha_f |j_p' I_f\rangle_{\text{s.p.}} + \sum \beta_f (j_1 \cdots j_m)$$

$$\times |j_1 j_2 \cdots j_m; I_f\rangle,$$

where the sum extends over all possible mixed configurations $|j_1 j_2 \cdots j_m; I\rangle$ and $|j; I\rangle_{\text{s.p.}}$ represents the extreme single-particle wave function. The nuclear matrix elements can then be written

$$\langle f \| \mathbf{T}_{KL\gamma\tau^+} \| i \rangle = \alpha \alpha_K \langle j \| \mathbf{T}_{KL\gamma\tau^+} \| j' \rangle_{\text{s.p.}}$$

$$[1 + \rho(KL\gamma)], \quad (12)$$

⁷ M. Rose and R. K. Osborn, Phys. Rev. **93**, 1326 (1954).

where one has

$$\rho(KL\gamma) = \frac{\sum \beta(j_\mu' j_\nu) b_K(j_\mu' j_\nu) \langle j_\nu \| \mathbf{T}_{KL\gamma\tau^+} \| j_\mu' \rangle}{\alpha \alpha_K \langle j \| \mathbf{T}_{KL\gamma\tau^+} \| j' \rangle_{\text{s.p.}}}. \quad (13)$$

In these last equations, the coefficients a_K and $b_K(j_\mu j_\nu)$ are geometrical decoupling factors and $\rho(KL\gamma)$ is a measure of the influence of the configuration mixing in terms of the single particle estimate.

With that formulation, the corrected nuclear-matrix-element ratios Λ_1 and Λ_2 can be written

$$\Lambda_1 = \Lambda_{1 \text{ s.p.}} \frac{1 + \rho(221)}{1 + \rho(220)}, \quad (14)$$

and

$$\Lambda_2 = \Lambda_{2 \text{ s.p.}} \frac{1 + \rho(321)}{1 + \rho(220)}. \quad (15)$$

An analysis of experimental data such as the comparative half-life ft , the beta-spectrum shape factor $C(W)$, and the longitudinal polarization of the beta particles $P_L(W)$ should give enough information to extract experimental values of Λ_1 and Λ_2 . The comparison of these values with their single-particle estimate gives valuable information about the amount of configuration mixing of the nuclear states involved in the decay and about the overlapping of their radial wave functions.

3. SPECTRUM SHAPE FACTOR, LONGITUDINAL POLARIZATION, AND ft VALUE

3.1. Standard Matrix Element and ft Value

It appears convenient to normalize the nuclear matrix elements to the standard

$$\eta = C_V \int \mathbf{R}_{ij} = - \left(\frac{8\pi}{5} \right)^{1/2} (2J_i + 1)^{-1/2}$$

$$\times \langle J_f \| C_V \mathbf{T}_{220\tau^+} \| J_i \rangle, \quad (16)$$

which can be computed from the corrected f_{el} value of

the beta transition by the relations

$$|\eta|^2 = \pi^3 \ln 2 / f_{cl},$$

$$f_{cl} = \int_1^{W_0} F(Z, W) p W (W_0 - W)^2 C(W) dW. \quad (17)$$

In these equations, t is the partial half-life of the decay, p and W are the momentum and the total energy of the beta particle, $C(W)$ is the spectrum shape factor, and $F(Z, W)$ is the Fermi function.

From Eq. (17) one has, taking $R_0 = 1.2 F$,

$$\left| \int \mathbf{R}_{ij} / R^2 \right| = 5.65 \times 10^6 \times A^{-2/3} \times (f_{cl})^{-1/2}. \quad (18)$$

3.2. Shape Factor and Longitudinal Polarization

Introducing the nuclear ratios Λ , Λ_1 , and Λ_2 defined in the previous section in the theoretical expression of the shape factor,⁴ we get, taking $C_A = -1.2 C_V$,

$$C(W) = \sum q^{4-2k} \{ A_{2K-1} [\frac{1}{2} \Lambda^2 \xi^2 L_{K-1} + (1 + 0.6\Lambda_1)^2 M_{K-1} + \Lambda \xi (1 + 0.6\Lambda_1) N_{K-1}] - 2q C_{2K-1} (1 - 0.6\Lambda_1) \times [(1 + 0.6\Lambda_1) N_{K-1} + \frac{1}{2} \Lambda \xi L_{K-1}] + q^2 D_{2K-1} (1 + 0.6\Lambda_1)^2 L_{K-1} + (0.04\Lambda_2^2 - 0.12\Lambda_1^2 - \Lambda \xi) q^2 B_{2K-1} L_{K-1} \}. \quad (19)$$

In that equation, A_{2K-1} , B_{2K-1} , C_{2K-1} , and D_{2K-1} are Greuling coefficients.⁸ $q = W_0 - W$ is the total energy of the neutrino associated with the decay. L_{K-1} , M_{K-1} , and N_{K-1} are linear combinations of radial electron wave functions and have been tabulated.⁹

The formula for the electron longitudinal polarization can be derived following the procedure of Lee-Whiting.¹⁰ It reads

$$P_L(W) = -C'(W)/C(W), \quad (20)$$

where $C'(W)$ is the "modified shape factor" and is obtained by substituting in $C(W)$:

$$L_{K-1} \rightarrow L_{K-1}^1 = (\rho^2 F_0 \rho^{2-2K})^{-1} g_{-K} f_K \sin(\Delta_{-K} - \Delta_K),$$

$$M_{K-1} \rightarrow M_{K-1}^1 = (\rho^2 F_0 \rho^{2-2K})^{-1} g_K f_{-K} \sin(\Delta_K - \Delta_{-K}),$$

$$N_{K-1} \rightarrow N_{K-1}^1 = (2\rho^2 F_0 \rho^{1-2K})^{-1} [g_K g_{-K} + f_K f_{-K}] \times \sin(\Delta_K - \Delta_{-K}),$$

where ρ is the nuclear radius; g_K and f_K are radial electron wave functions and Δ_K are their phase shifts.

3.3. ξ Approximation

By expanding the electron radial functions in powers of the radius r and evaluating the value of their leading term at the nuclear surface, one gets for the spectrum

⁸ E. Greuling, Phys. Rev. **61**, 568 (1942).

⁹ C. P. Bhalla and M. E. Rose, Oak Ridge National Laboratory Report No. ORNL-3207, 1961 (unpublished).

¹⁰ G. E. Lee-Whiting, Can. J. Phys. **36**, 252 (1958).

TABLE III. Experimental data on the nonunique second-forbidden transitions [A_{exp}^2 is the experimental value derived by fitting the shape factor to Eq. (21). $\log(ft)_a$ is not corrected for the forbidden shape of the beta spectrum.]

| Mother isotope | I_i | I_F | W_0 | A_{exp}^2 | $\log(ft)_a$ |
|-----------------------------|-----------------|-----------------|-------|--------------------|--------------|
| $^{17}\text{Cl}_{19}^{86}$ | 2+ | 0+ | 2.4 | 0.6 ± 0.1 | 13.3 |
| $^{26}\text{Fe}_{33}^{59}$ | $\frac{3}{2}^-$ | $\frac{7}{2}^-$ | 4.07 | 3.3 ± 0.7 | 10.9 |
| $^{43}\text{Tc}_{56}^{99}$ | $\frac{3}{2}^+$ | $\frac{5}{2}^+$ | 1.57 | 2.0 ± 0.5 | 12.3 |
| $^{53}\text{I}_{76}^{129}$ | $\frac{7}{2}^+$ | $\frac{3}{2}^+$ | 1.29 | 10 \pm 1 | 13.5 |
| $^{55}\text{Cs}_{80}^{135}$ | $\frac{3}{2}^+$ | $\frac{3}{2}^+$ | 1.41 | 10 \pm 1 | 13.2 |
| $^{55}\text{Cs}_{82}^{137}$ | $\frac{3}{2}^+$ | $\frac{3}{2}^+$ | 3.31 | 40 $_{-25}^{+60}$ | 11.8 |

shape factor of second-forbidden beta transitions:

$$C(W) = A^2 (W_0 - W)^2 + (W^2 - 1) \quad (21)$$

with

$$A^2 = [(2 - \Lambda + 1.2\Lambda_1) / (1 - \Lambda + 0.6\Lambda_1)]^2. \quad (22)$$

The experimental data have usually been fitted to this particular dependence, and in this approximation, the contribution of $\int \mathbf{S}_{ijk}$ is completely neglected. Although the comparison of such an expression with model-dependent values of Λ and Λ_1 is instructive, it seems preferable to use the theoretical expression of $C(W)$ given by Eq. (19) and introduce in it the electron wave functions computed from the potential of an extended nuclear charge distribution and corrected for screening.

4. EXPERIMENTAL DATA AND MATRIX ELEMENTS IN THE DECAY OF Cl^{36} , Fe^{59} , Tc^{99} , I^{129} , Cs^{135} , AND Cs^{137}

4.1. Experimental Data

Six nonunique second-forbidden beta transitions allow reliable shape-factor measurements and have been investigated by several experimental groups.¹¹⁻¹⁹ They are: Cl^{36} , Fe^{59} , Tc^{99} , I^{129} , Cs^{135} , and Cs^{137} . Their shape factors have been given in terms of Eq. (21). Table III summarizes the averaged experimental results.

4.2. Matrix Element Ratios Compatible with the Experimental Data

In order to determine the values of the parameters Λ , Λ_1 , Λ_2 , compatible with the experimental shape factors, we have done a χ^2 analysis with the following relation:

$$Q^2(\Lambda, \Lambda_1, \Lambda_2) = \sum \left[\frac{C_{\text{th}}(W_i) - C_{\text{exp}}(W_i)}{\Delta C_{\text{exp}}(W_i)} \right]^2. \quad (23)$$

¹¹ R. G. Johnson, O. E. Johnson, and L. M. Langer, Phys. Rev. **102**, 1142 (1956).

¹² L. Feldman and C. S. Wu, Phys. Rev. **87**, 1091 (1952).

¹³ F. R. Metzger, Phys. Rev. **88**, 1360 (1952).

¹⁴ D. E. Wortman and L. M. Langer, Phys. Rev. **131**, 325 (1963).

¹⁵ E. der Mateosian and C. S. Wu, Phys. Rev. **91**, 497 (1953).

¹⁶ L. Lidofsky, E. Alperovitch, and C. S. Wu, Phys. Rev. **90**, 387 (1953).

¹⁷ L. M. Langer and R. J. D. Moffat, Phys. Rev. **82**, 635 (1951).

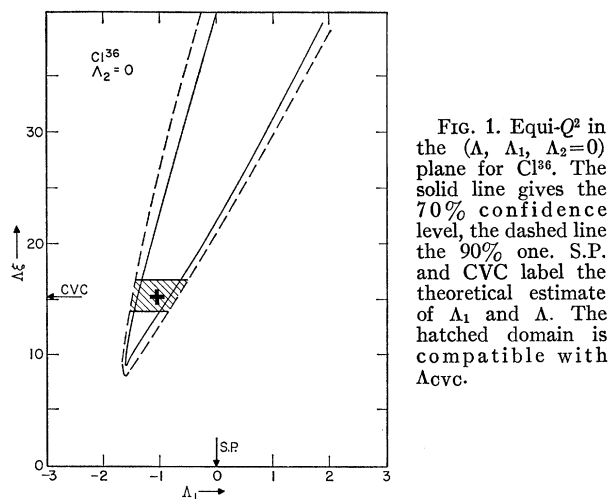


FIG. 1. Equi- Q^2 in the $(\Delta, \Delta_1, \Delta_2=0)$ plane for Cl^{36} . The solid line gives the 70% confidence level, the dashed line the 90% one. S.P. and CVC label the theoretical estimate of Δ_1 and Δ . The hatched domain is compatible with Δ_{CVC} .

In that equation, $C_{\text{th}}(W_i)$ is the value resulting from the Eq. (19). $C_{\text{exp}}(W_i)$ and $\Delta C_{\text{exp}}(W_i)$ are the experimental values and errors of the shape factor, as a function of the beta particle energy W_i .

We have plotted in the plane (Δ, Δ_1) equi- Q^2 as a function of Δ_2 . A variation of Δ_2 between 0 and 10 results in a nonsignificant displacement of the equi- Q^2 , so that one can set $\Delta_2=0$ to simplify the general discussion of the solutions Δ and Δ_1 . In Figs. 1–6, we give the equi- Q^2 in the plane $(\Delta, \Delta_1, \Delta_2=0)$ corresponding to the confidence levels of 70% and 90%, respectively. [$P(\chi^2 > Q^2) = 0.3$ and 0.1, respectively.]

The relatively broad range of the possible values Δ and Δ_1 can be limited if one accepts the prediction Δ_{CVC}

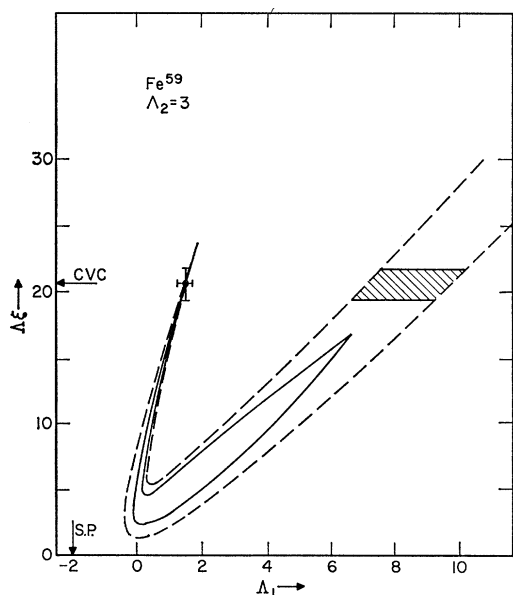


FIG. 2. Equi- Q^2 in the $(\Delta, \Delta_1, \Delta_2=3)$ plane for Fe^{59} . The solid line gives the 70% confidence level, the dashed line the 90% one. S.P. and CVC label the theoretical estimate of Δ_1 and Δ . The hatched domain is compatible with Δ_{CVC} .

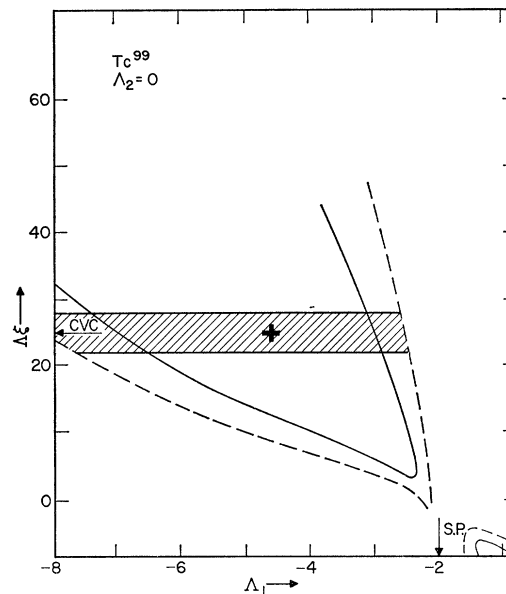


FIG. 3. Equi- Q^2 in the $(\Delta, \Delta_1, \Delta_2=0)$ plane for Tc^{99} . The solid line gives the 70% confidence level, the dashed line the 90% one. S.P. and CVC label the theoretical estimate of Δ_1 and Δ . The hatched domain is compatible with Δ_{CVC} .

given by the conserved vector-current theory.⁶ With the present status of the experiments performed to test the validity of the CVC hypothesis in beta decay,²⁰

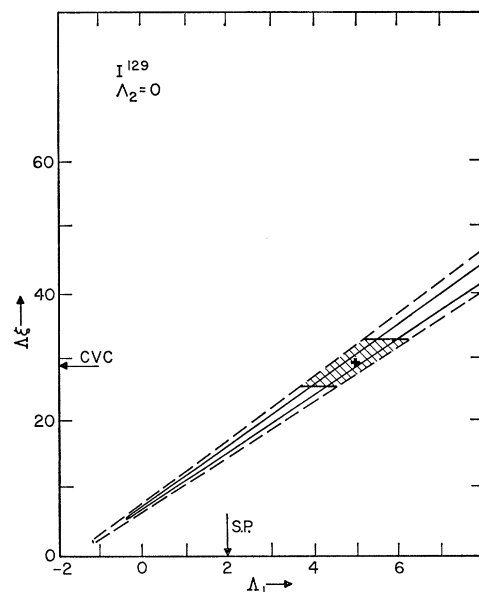


FIG. 4. Equi- Q^2 in the $(\Delta, \Delta_1, \Delta_2=0)$ plane for I^{129} . The solid line gives the 70% confidence level, the dashed line the 90% one. S.P. and CVC label the theoretical estimate of Δ_1 and Δ . The hatched domain is compatible with Δ_{CVC} .

¹⁸ I. Yoshizawa, Nucl. Phys. **5**, 122 (1958).

¹⁹ H. Daniel and H. Schmitt, Z. Physik. **168**, 292 (1962).

²⁰ C. S. Wu, Rev. Mod. Phys. **36**, 618 (1964).

and the experimental ratios of matrix elements

$$\langle J_f || \gamma_s T_{K,L-1,1} || J_i \rangle / \langle J_f || T_{K,L,0} || J_i \rangle$$

derived from first-forbidden beta transitions,^{21,22} a relative error of 10% on the theoretical value Λ_{CVC} seems to be a safe limit. Under that assumption, one can derive experimental values of Λ_1 from the computed Q^2 analysis.

In Table IV we give the shell-model configurations and the theoretical estimates of the nuclear-matrix-element ratios for the beta transitions considered. The experimental value $\Lambda_{1 \text{ exp}}$ is obtained setting $\Lambda = \Lambda_{\text{CVC}}$ and $\Lambda_2 = 0$ in Eq. (19). The Coulomb energy factor ξ has been computed with the nuclear radius $R = 1.2 \times A^{1/3}$ F and is given in units of $\hbar = m = c = 1$ by

$$\xi = 1.175 \times Z \times A^{-1/3},$$

where Z and A are the nuclear charge and mass number, respectively.

The comparison of $\Lambda_{1 \text{ exp}}$ with $\Lambda_{1 \text{ S.P.}}$ given in Table IV shows that the extreme shell model description leads

TABLE 4. Shell-model configurations, theoretical estimates of the matrix element ratios, and experimental values compatible with the CVC theory.

| Isotope | $ p\rangle$ | $ n\rangle$ | $\Lambda_{\text{CVC}}\xi$ | $\Lambda_{1 \text{ S.P.}}$ | $\Lambda_{2 \text{ S.P.}}$ | $\Lambda_{1 \text{ exp}}$ |
|------------------------|-------------|-------------|---------------------------|----------------------------|----------------------------|--|
| $^{17}\text{Cl}^{86}$ | $d_{3/2}$ | $d_{3/2}$ | 15.4 | 0 | 0 | $-1.1_{-0.5}^{+0.4}$ |
| $^{26}\text{Fe}^{59}$ | $f_{7/2}$ | $p_{3/2}$ | 21.2 | -2 | +3 | $\begin{cases} +1.65 \pm 0.25^a \\ -2.0 \pm 0.2^b \end{cases}$ |
| $^{43}\text{Tc}^{99}$ | $g_{9/2}$ | $d_{5/2}$ | 25.8 | -2 | +2.6 | $-4.6_{-1.7}^{+2.5}$ |
| $^{53}\text{I}^{129}$ | $g_{7/2}$ | $d_{3/2}$ | 28.8 | +2 | -1 | $+5.2 \pm 1.0$ |
| $^{55}\text{Cs}^{135}$ | $g_{7/2}$ | $d_{3/2}$ | 29.4 | +2 | -1 | $+5.0 \pm 0.85$ |
| $^{55}\text{Cs}^{137}$ | $g_{7/2}$ | $d_{3/2}$ | 31.2 | +2 | -1 | $+2.9 \pm 0.4$ |

^a See Ref. 14.

^b See Ref. 13.

to the right magnitude and sign of Λ_1 , with the exception of Fe^{59} . In that particular case, there is a disagreement between experimental data from different groups.^{13,14} Langer *et al.*¹⁴ find a shape factor consistent with the ξ approximation. Because of the relatively high endpoint energy of that particular beta transition ($W_0 = 4.07$, $\xi = 7.85$), the ξ approximation ($\xi \gg W_0$) might be poor. If the results of Metzger *et al.*¹³ apply, an excellent agreement with the shell-model prediction is obtained: $\Lambda_{1 \text{ exp}} = -2.0 \pm 0.2$, $\Lambda_{2 \text{ exp}} = 1.0 \pm 0.5$. Figure 7 shows a comparison of the theoretical fit to both experimental results.

The case of Cs^{137} is the most interesting one. The shell-model prediction gives a vanishing contribution of the term in $(W^2 - 1)$ of Eq. (21), which is experimentally verified. In Fig. 6, two distinct regions of sets (Λ, Λ_1) are shown from the equi- Q^2 giving the 90% confidence level. The island between these two regions disappears as Λ_2 is increased. Although the choices of (Λ, Λ_1) centered around $\Lambda_{1 \text{ exp}}$ and $\Lambda_{1 \text{ S.P.}}$ give roughly the

²¹ P. Lipnik and J. W. Sunier, Nucl. Phys. **53**, 305 (1964).

²² P. Lipnik and J. W. Sunier, Nucl. Phys. **65**, 21 (1965).

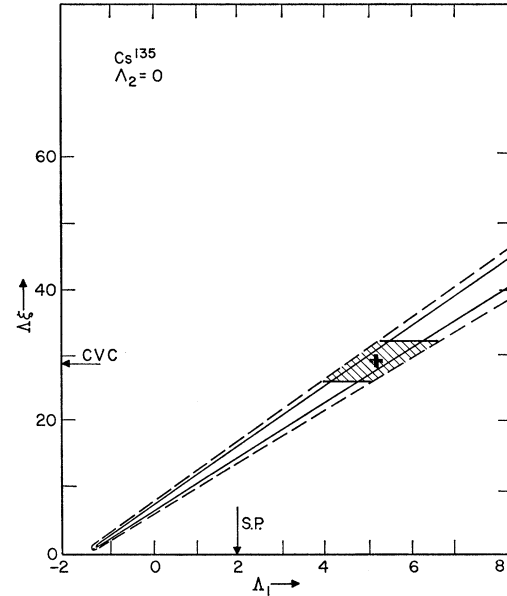


FIG. 5. Equi- Q^2 in the $(\Lambda, \Lambda_1, \Lambda_2=0)$ plane for Cs^{135} . The solid line gives the 70% confidence level, the dashed line the 90% one. S.P. and CVC label the theoretical estimate of Λ_1 and Λ . The hatched domain is compatible with Λ_{CVC} .

same fit of the shape-factor measurement, the behavior of the longitudinal polarization is quite different, as is shown in Fig. 8. The similarity between the spectrum shape factors of the Cs^{137} and RaE decays is striking. A measurement of the energy dependence of the electron longitudinal polarization in the decay of Cs^{137} would be

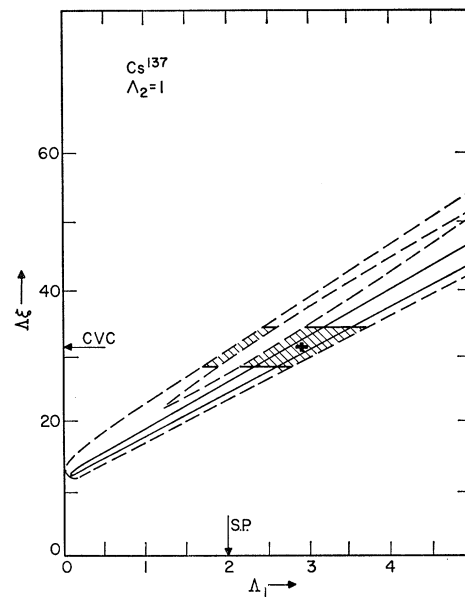


FIG. 6. Equi- Q^2 in the $(\Lambda, \Lambda_1, \Lambda_2=1)$ plane for Cs^{137} . The solid line gives the 70% confidence level, the dashed line the 90% one. S.P. and CVC label the theoretical estimate of Λ_1 and Λ . The hatched domain is compatible with Λ_{CVC} .

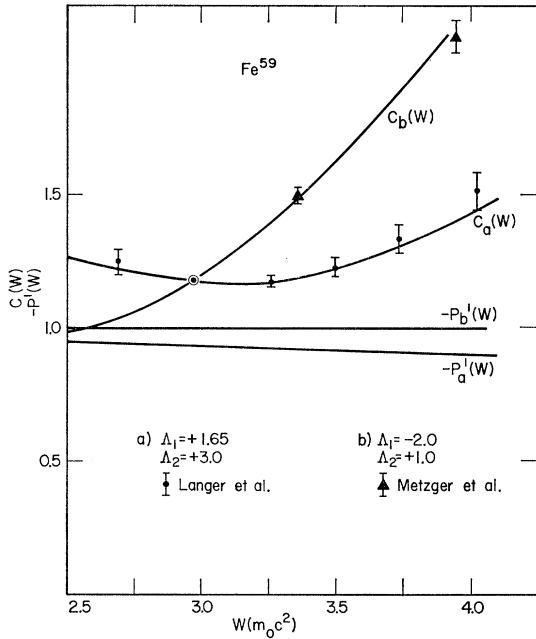


FIG. 7. Shape factor $C(W)$ and reduced electron longitudinal polarization $-P^1(W) = P_L(W)W/\rho$ for Fe^{59} , as a function of the electron energy W .

highly desirable. It could give the additional information required to compute a precise set of nuclear parameters.

5. CONFIGURATION MIXING AND RADIAL MATRIX ELEMENTS

Let us make some comments concerning Eqs. (7) to (14) of Sec. 2. The value $\Lambda_{1 \text{ s.p.}}$ does not change if one

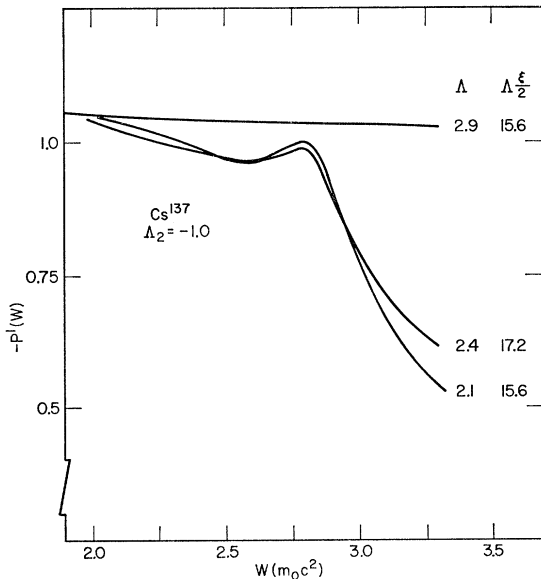


FIG. 8. Reduced electron longitudinal polarization of Cs^{137} beta decay as a function of the electron energy W .

TABLE V. Experimental values of the mixing parameter $\rho(220)$.

| Isotope | Extreme shell model j | Extreme shell model j' | Admixture $\rho(221)/\rho(220)$ | $\rho_{\text{exp}}(220)$ | |
|------------|-------------------------|--------------------------|---------------------------------|--------------------------|--|
| C^{186} | $(d_{3/2})_p^1$ | $(d_{3/2})_n^3$ | $(s_{1/2})_p$ | a | -0.27 |
| Fe^{59} | $(f_{7/2})_p^6$ | $(p_{3/2})_n^3$ | $(f_{5/2})_n$ | $+1/2$ | 0.0 ^b -0.42 ^c |
| Tc^{99} | $(g_{9/2})_p^3$ | $(d_{5/2})_n^6$ | $(g_{7/2})_n$ | $-9/2$ | -0.19 |
| I^{129} | $(g_{7/2})_p^3$ | $(d_{3/2})_n^2$ | $(d_{5/2})_p$ | $-3/2$ | -0.31 |
| Cs^{135} | $(g_{7/2})_p^5$ | $(d_{3/2})_n^2$ | $(d_{5/2})_p$ | $-5/2$ | -0.30 |
| Cs^{137} | $(g_{7/2})_p^5$ | $(d_{3/2})_n^4$ | $(d_{5/2})_p$ | $-5/2$ | -0.11 |

^a In that case, Eq. (14) is not valid and has to be replaced by $\Lambda_1 = 3\rho(220)/[1 + \rho(220)]$, the single-particle value being $\Lambda_{1 \text{ s.p.}} = 0$.
^b See Ref. 13.
^c See Ref. 14.

considers higher orders of seniority in the configurations j and j' , because then $\rho(221) = \rho(220)$. Eqs. (12) to (15) simplify the computation considerably because a limited number of configurations j'_μ and j'_ν lead to nonvanishing reduced matrix elements $\langle j'_\nu || \mathbf{T}_{KL\gamma} || j'_\mu \rangle$. In that sense, the ratio of the experimental values $\Lambda_{1 \text{ exp}}$ and $\Lambda_{2 \text{ exp}}$ (Table IV) to their extreme single-shell-model estimate $\Lambda_{1 \text{ s.p.}}$ and $\Lambda_{2 \text{ s.p.}}$ (Table IV) is a measure of the amount of configuration mixing.

Theoretically, these ratios can be computed with Eqs. (11) to (15) as functions of overlapping integrals between the radial wave functions of the initial and final nuclear states. Such computations are tedious if more than two or three shell-model orbits are mixed to compose the wave functions of these states. In the following we shall restrict ourselves to the mixing of three shell-model wave functions and consider this procedure as a qualitative attempt to interpret the experimental data.

5.1. Computation of the Parameter $\rho(220)$

With the simplification discussed above, the nuclear matrix elements given by Eq. (12) reduce to a sum of two single-particle matrix elements and take the form:

$$\langle j || \mathbf{T}_{KL\gamma} \tau^+ || i \rangle = \alpha a_2 \langle j || \mathbf{T}_{KL\gamma} || j'_{\text{s.p.}} \rangle + \beta b_2 \langle j_1 j_1 \rangle \times \langle j_1 || \mathbf{T}_{KL\gamma} || j_1' \rangle_{\text{s.p.}} \quad (24)$$

In $\mathbf{T}_{KL\gamma}$ Eq. (23), the primed momenta label the neutron states.

TABLE VI. Radial integrals^a for the harmonic oscillator potential. $F_L = \int r^{L+2} R(r) R'(r) dr = \langle N'l | r^L | N'l' \rangle$. The value of b_0/R is that of Wahlborn.^b

| N' | l' | F_2 |
|-----------|-----------|---|
| N | l | $[N + \frac{3}{2}] b_0^2$ |
| $N \pm 2$ | l | $-\frac{1}{2} [(N+l+2 \pm 1)(N-l+1 \pm 1)]^{1/2} b_0^2$ |
| $N \pm 2$ | $l \pm 2$ | $\frac{1}{2} [(N+l+1 \pm 2)(N+l+3 \pm 1)]^{1/2} b_0^2$ |
| N | $l \pm 2$ | $-\frac{1}{2} [(N+l+2 \pm 1)(N-l+1 \mp 1)]^{1/2} b_0^2$ |
| $N \mp 2$ | $l \pm 2$ | $\frac{1}{2} [(N-l \mp 2)(N-l+2 \mp 2)]^{1/2} b_0^2$ |

$b_0 = (\hbar/M\omega_0)^{1/2}$; $b_0/R = 0.82 \times A^{-1/6}$ ($\hbar = m = c = 1$)

^a W. H. Shaffer, Rev. Mod. Phys. 16, 245 (1944).
^b S. Wahlborn, Nucl. Phys. 8, 209 (1964).

TABLE VII. Standard matrix elements compared to their single-particle estimate.

| Isotope | $\log f t$ | $ \mathcal{R}_{ij}/R^2 _{\text{exp}}$ | a_2 | $\langle j T_{220}\tau^+ j' \rangle$ | $ \mathcal{R}_{ij}/R^2 _{\text{s.p.}}$ | α_{eff} |
|-------------------------------|------------|---------------------------------------|----------|--|--|-----------------------|
| Cl ³⁶ | 15.8±0.3 | 0.007±0.001 | 1 | $(7/2\sqrt{\pi})b_0^2$ | 0.084 | 0.083 |
| Fe ⁵⁹ ^a | 12.5±0.2 | 0.210±0.020 | 1 | $(6/\sqrt{\pi})b_0^2$ | 0.218 | 0.965 |
| ^b | 13.4±0.3 | 0.074±0.011 | 1 | $(6/\sqrt{\pi})b_0^2$ | 0.377 | 0.196 |
| Tc ⁹⁹ | 14.3±0.4 | 0.019±0.004 | (1/2√15) | $[9\sqrt{(10/7\pi)}]b_0^2$ | 0.038 | 0.200 |
| I ¹²⁹ | 14.6±0.2 | 0.011±0.002 | (1/4√2) | $[18/\sqrt{(7\pi)}]b_0^2$ | 0.046 | 0.239 |
| Cs ¹³⁵ | 14.5±0.2 | 0.012±0.002 | (1/4√2) | $[18/\sqrt{(7\pi)}]b_0^2$ | 0.048 | 0.250 |
| Cs ¹³⁷ | 13.9±0.4 | 0.024±0.005 | (1/4√2) | $[18/\sqrt{(7\pi)}]b_0^2$ | 0.061 | 0.394 |

^a See Ref. 14.

^b See Ref. 13.

Using Eq. (7), Eq. (10), and Table II, we can compute

$$\frac{\rho(221)}{\rho(220)} = \frac{\langle j_1||\mathbf{T}_{221}||j_1' \rangle \langle j||\mathbf{T}_{220}||j' \rangle}{\langle j_1||\mathbf{T}_{220}||j_1' \rangle \langle j||\mathbf{T}_{221}||j' \rangle}$$

and the parameter $\rho(220)$ can be extracted from Eq. (14) as a function of $\Lambda_1/\Lambda_{1 \text{ s.p.}}$. The experimental values $\rho_{\text{exp}}(220)$ computed with the parameter $\Lambda_{1 \text{ exp}}$ discussed under Sec. 4.2 are given in Table V. In the same table we give also the shell-model configurations j, j', j_1, j_1' and the corresponding ratio $\rho(221)/\rho(220)$.

5.2. Standard Matrix Elements Compared to Their Single-Particle Estimate

The standard matrix element, computed from the comparative half-life of the decay according to Eq. (17), is smaller than its extreme single-particle value. Considering Eqs. (7), (12), (16), and (17), we define an effective reduction factor

$$\alpha_{\text{eff}} = \frac{\langle f||T_{220}\tau^+||i \rangle_{\text{exp}}}{[1 + \rho_{\text{exp}}(220)]a_2 \langle j||T_{220}\tau^+||j' \rangle_{\text{s.p.}}} \quad (25)$$

The geometrical decoupling factor a_2 can be evaluated by considering only the lowest order of seniority in the configuration jj' . The single-particle matrix element $\langle j||T_{220}\tau^+||j' \rangle$ depends on the radial integral $F_2(jj')$ which we compute from Table VI, giving the solutions for the harmonic oscillator potential. The results are summarized in Table VII, in which we give the experimental standard matrix element $|\mathcal{R}_{ij}/R^2|$, the corrected comparative half-life, the geometrical factor a_2 , and the reduction factor α_{eff} with respect to the single-particle estimate:

$$\left| \frac{\mathcal{R}_{ij}}{R^2} \right|_{\text{s.p.}} = \left(\frac{8\pi}{5} \right)^{1/2} (2J_i + 1)^{-1/2} a_2 \times [1 + \rho_{\text{exp}}(220)] \langle j||T_{220}\tau^+||j' \rangle. \quad (20)$$

6. DISCUSSION OF RESULTS

The nuclear matrix element ratios $\Lambda\xi = -\mathcal{I}i\mathbf{A}_{ij}/\mathcal{I}\mathbf{R}_{ij}$ and $\Lambda_1 = \mathcal{I}i\mathbf{T}_{ij}/\mathcal{I}\mathbf{R}_{ij}$ compatible with the shape factors investigated agree with the prediction Λ_{CVC} of

the conserved vector-current theory and exhibit reasonable deviations from the single particle estimate $\Lambda_{1 \text{ s.p.}}$. The matrix element $\mathcal{I}\mathbf{S}_{ijk}$ has small influence on the shape factor and can be neglected. Even in the case of Fe⁵⁹, the deviations from the ξ approximation, suggested by the shape factor measurement of Metzger *et al.*,¹³ can be accounted for by taking further terms in the expansion of the transition probability as a function of ξ .

The deviations from $\Lambda_{1 \text{ s.p.}}$ can be explained by a relatively small amount of configuration mixing in the shell-model wave functions (10–30%). The correction, measured by the parameter $\rho_{\text{exp}}(220)$ is a minimum for the decay of Tc⁹⁹ and Cs¹³⁷, as could be expected from the shell-model level structure.

The standard matrix element $|\mathcal{R}_{ij}/R^2|$ is reduced with respect to its single-particle estimate. The reduction factor decreases from 5 to 2.5 as the neutrons fill the levels of the $N=82$ shell between Tc⁹⁹ and Cs¹³⁷. The standard matrix element of the Cl³⁶ transition is reduced by a factor of 12, although configuration mixing does not seem prohibitive in that case. The (f, t) value resulting from the shape factor measurement of Langer *et al.*¹⁴ is surprisingly low. The analysis of the measurement of Metzger *et al.*¹³ agrees much better with ($\Lambda_{\text{CVC}}, \Lambda_{1 \text{ s.p.}}$) and the general trends exhibited by all other second forbidden transitions. It is therefore not improbable that the ξ approximation is not sufficient to describe the shape factor of that particular transition.

A comparison of the similar transitions in the decays of Cs¹³⁷, Cs¹³⁵, and I¹²⁹ is instructive in many aspects. First, the reduction factors α_{eff} of the standard matrix elements are proportional within $\pm 8\%$ to the statistical factor $[N_n \times (N_p + 1)]^{1/2}$, where N_n and N_p are the number of nucleons in the $(d_{3/2})_n$ and $(g_{3/2})_p$ levels of the initial state. This fact supports our approximation that only pure $(d_{3/2})_n$ configurations are involved in these decays. With this in mind, one can evaluate the ratio of the amplitudes of the nuclear wave functions. Considering the states of seniority 1 and 3 only, one can write according to Eq. (11):

$$|i\rangle = \alpha_i \left| \left(\frac{7}{2} \right)_p^{5/2} \left(\frac{3}{2} \right)_n^{40} \right\rangle + \beta_i \left| \left(\frac{7}{2} \right)_p^{42} \left(\frac{5}{2} \right)_p^{15} \left(\frac{3}{2} \right)_n^{40} \right\rangle + \left(\frac{7}{2} \right)_p,$$

$$|f\rangle = \alpha_f \left| \left(\frac{3}{2} \right)_p^{60} \left(\frac{3}{2} \right)_n^{3/2} \right\rangle + \beta_f \left| \left(\frac{3}{2} \right)_p^{42} \left(\frac{5}{2} \right)_p^{20} \left(\frac{3}{2} \right)_n^{3/2} \right\rangle + \left(\frac{3}{2} \right)_p.$$

The nuclear matrix element then takes the form

$$\langle f || T_{220}\tau^+ || i \rangle = \alpha_i \alpha_f (32)^{-1/2} \langle g_{7/2} || T_{220}\tau^+ || d_{3/2} \rangle \\ + \beta_i \beta_f 2(35)^{-1/2} \langle d_{5/2} || T_{220}\tau^+ || d_{3/2} \rangle,$$

from which one gets, considering Eq. (7), Eq. (13), and Table VI:

$$\beta_i \beta_f / \alpha_i \alpha_f = 1.01 \rho(220).$$

In the case of Cs¹³⁷, the experimental value $\rho_{\text{exp}}(220) = -0.11$ and the cancellation between the matrix elements occurring in the leading term in p^2 of the theoretical shape-factor distribution confirms the almost single-particle character of the beta transition.

The experimental value Λ_1 , derived for the decay of Cl³⁶, indicates a considerable mixing of ($d_{3/2}$) and ($s_{1/2}$) orbits in the initial wave function. Pure ($d_{3/2}$) configuration would imply $\Lambda_1 \equiv 0$ for the β^- decay of Cl³⁶ into S³⁶ as well as for the transition of Cl³⁶ into Ar³⁶ by electron capture. This contradicts the experimental results²³:

$$\Lambda_1(\beta^-) = -1.1 \pm 0.5, \quad \Lambda_1(e.c.) = -0.35 \pm 0.10.$$

²³ P. Lipnik, G. Pralong, and J. W. Sunier, Nucl. Phys. **59**, 504 (1964).

We consider the wave functions

$$\text{Cl}^{36} | i \rangle = \alpha_i | (d_{3/2})_p^1 (d_{3/2})_n^3; 2 \rangle \\ + \beta_i | (d_{3/2})_p^2 (s_{1/2})_p^{-1} (d_{3/2})_n^3; 2 \rangle,$$

$$\text{Ar}^{36} | f \rangle = \alpha_f | (d_{3/2})_p^2 (d_{3/2})_n^2; 0 \rangle.$$

Application of Eq. (7), Eq. (13), and Table VI gives

$$\beta_i / \alpha_i = (7/4\sqrt{5})\rho(220) = -0.21.$$

This relative amount of $|(s_{1/2})_p^{3/2} \frac{1}{2} (d_{3/2})_n^{5/2} \frac{1}{2}; J=2, T=1\rangle$ to $|(s_{1/2})_p^0 (d_{3/2})_n^4; J=2, T=1\rangle$ configuration agrees very well with the value $\beta_i / \alpha_i = -0.23$ reported by Lovas *et al.*²⁴ in their study of the excited states of Cl³⁶ and Ar³⁶.

In conclusion, we would like to stress that, despite the limited number of observables and experimental data, the second-forbidden beta transitions agree fairly well with the j - j coupling model, in a consistent manner. Although this agreement may be partially of a qualitative nature, a systematic study of observables like the electron longitudinal polarization and its energy dependence could be very promising and would allow a more precise determination of the relevant nuclear parameters.

²⁴ I. Lovas and J. Révai, Nucl. Phys. **59**, 364 (1964).

Nuclear Recoil in the C¹²(p, pn)C¹¹ Reaction.* I. Angular Distribution

J. A. PANONTIN,† L. L. SCHWARTZ,‡ A. F. STEHNEY, E. P. STEINBERG, AND L. WINSBERG§

Argonne National Laboratory, Argonne, Illinois

(Received 27 December 1965)

The angular distribution of the recoiling C¹¹ atoms from the reaction C¹²(p, pn)C¹¹, induced by 450-MeV protons, was measured. The results were compared with the theoretical calculations of Benioff and Person. The distorted-wave impulse approximation gives better agreement than does the plane-wave approximation. However, the theoretical values from both calculations appear to be too large at the backward angles. This may indicate the existence of competing mechanisms. The results reported here are in general agreement with the thick-target thick-catcher recoil measurements of Singh and Alexander. A similar comparison for the reaction Cu⁶⁵(p, pn)Cu⁶⁴ indicates no agreement between the two types of experiment.

INTRODUCTION

THE measurement of the angular and energy distribution of recoiling atoms from the (p, pn), ($p, 2p$), and other simple reactions provides information about the mechanism of nuclear reactions and about the structure of the target nucleus.¹ Measurements of the simple reactions are expected to be more sensitive to the

nature of initial encounter between the incident proton and the target nucleus than reactions in which many particles are emitted. Hence, these reactions are being extensively investigated.²

The C¹²(p, pn)C¹¹ reaction was chosen for this type of study because C¹² is a closed-shell nucleus of relatively simple structure. Furthermore, the amount of C¹¹ formed in this reaction can be readily determined by measuring the intensity of positrons emitted during radioactive decay.

Measurements of the recoiling C¹¹ atoms from this reaction have previously been made by Singh and

* This work was done under the auspices of the U. S. Atomic Energy Commission.

† Present address: Purdue University, Lafayette, Indiana.

‡ Present address: Lawrence Radiation Laboratory, University of California, Livermore, California.

§ Present address: University of Illinois at Chicago Circle, Chicago, Illinois.

¹ P. Benioff and L. Person, Phys. Rev. **140**, B844 (1965).

² J. R. Grover and A. A. Caretto, Ann. Rev. Nucl. Sci. **14**, 51 (1964).